


Peptostreptococcus anaerobius promotes colorectal carcinogenesis and modulates tumour immunity

Xiaohang Long^{1,2,3}, Chi Chun Wong^{1,2,3}, Li Tong^{1,2,3}, Eagle S. H. Chu^{1,2,3}, Chun Ho Szeto^{1,2,3}, Minne Y. Y. Go^{1,2,3}, Olabisi Oluwabukola Coker^{1,2,3}, Anthony W. H. Chan⁴, Francis K. L. Chan^{1,2,3}, Joseph J. Y. Sung^{1,2,3} and Jun Yu^{1,2,3*} 

Emerging evidence implicates a role of the gut microbiota in colorectal cancer (CRC). *Peptostreptococcus anaerobius* (*P. anaerobius*) is an anaerobic bacterium selectively enriched in the faecal and mucosal microbiota from patients with CRC, but its causative role and molecular mechanism in promoting tumorigenesis remain unestablished. We demonstrate that *P. anaerobius* adheres to the CRC mucosa and accelerates CRC development in *Apc*^{Min/+} mice. In vitro assays and transmission electron microscopy revealed that *P. anaerobius* selectively adheres to CRC cell lines (HT-29 and Caco-2) compared to normal colonic epithelial cells (NCM460). We identified a *P. anaerobius* surface protein, putative cell wall binding repeat 2 (PCWBR2), which directly interacts with colonic cell lines via α_2/β_1 integrin, a receptor frequently overexpressed in human CRC tumours and cell lines. Interaction between PCWBR2 and integrin α_2/β_1 induces the activation of the PI3K–Akt pathway in CRC cells via phospho-focal adhesion kinase, leading to increased cell proliferation and nuclear factor kappa-light-chain-enhancer of activated B cells (NF- κ B) activation. NF- κ B in turn triggers a pro-inflammatory response as indicated by increased levels of cytokines, such as interleukin-10 and interferon- γ in the tumours of *P. anaerobius*-treated *Apc*^{Min/+} mice. Analyses of tumour-infiltrating immune cell populations in *P. anaerobius*-treated *Apc*^{Min/+} mice revealed significant expansion of myeloid-derived suppressor cells, tumour-associated macrophages and granulocytic tumour-associated neutrophils, which are associated with chronic inflammation and tumour progression. Blockade of integrin α_2/β_1 by RGDS peptide, small interfering RNA or antibodies all impair *P. anaerobius* attachment and abolish *P. anaerobius*-mediated oncogenic response in vitro and in vivo. Collectively, we show that *P. anaerobius* drives CRC via a PCWBR2–integrin α_2/β_1 –PI3K–Akt–NF- κ B signalling axis and identify the PCWBR2–integrin α_2/β_1 axis as a potential therapeutic target for CRC.

Colorectal cancer (CRC) is one of the most common cancers worldwide¹. The initiation and progression of CRC involve the complex interplay between genetic, epigenetic and environmental factors, the latter being the predominant trigger for CRC². Emerging evidence indicates that gut microbes might be an important environmental factor that promotes CRC development^{3,4}. Large-scale metagenomic studies have demonstrated that both mucosal and stool microbiota composition in CRC patients are distinct from healthy individuals^{5,6}. Microbial dysbiosis plays an important role in the aetiology of CRC and has been shown to modulate the pathological functions associated with CRC, including cell proliferation, apoptosis and immune response^{7–10}. Several ‘driver’ bacteria, such as enterotoxigenic *Bacteroides fragilis*¹¹ and *Fusobacterium nucleatum* (*F. nucleatum*)¹² have been found to be associated with CRC development. These microbes can promote tumour development through direct interaction with host cancer cells¹³, secretion of oncogenic virulence factors^{11,14} or generation of carcinogenic microbial metabolites¹⁵. Hence, the identification and characterization of driver bacteria associated with CRC is urgent and important.

To identify the microbial species associated with CRC, we recently conducted two large-scale characterizations of CRC faecal and mucosal microbiota composition using metagenomic and 16S recombinant DNA sequencing, respectively^{5,6}. Our work led to the discovery

of bacterial strains enriched in CRC or adenomas, including known CRC-associated *F. nucleatum* and *Peptostreptococcus stomatis*. We also identified *Peptostreptococcus anaerobius* (*P. anaerobius*) as a bacterium selectively enriched in the stools and mucosa of CRC patients. *P. anaerobius* is a gram-positive anaerobic bacterium that normally resides in the oral cavity and gut¹⁶. We further demonstrated that *P. anaerobius* could promote colonic dysplasia in mice treated with azoxymethane, and that this bacterium induces cholesterol biosynthesis to support increased colonic cell proliferation¹⁷. However, the role of *P. anaerobius* in spontaneous CRC and its molecular mechanism in driving tumorigenesis remain poorly understood.

In this study, we investigated the effects and molecular mechanisms of *P. anaerobius* on spontaneous CRC formation and progression in mice. We found that *P. anaerobius* promotes CRC development in *Apc*^{Min/+} mice. *P. anaerobius* mediates this effect via its surface protein, putative cell wall binding repeat 2 (PCWBR2), which directly interacts with epithelial cell receptor integrin α_2/β_1 to initiate a PI3K–Akt–nuclear factor kappa-light-chain-enhancer of activated B cells (NF- κ B) cascade, which in turn promotes cell proliferation and a pro-inflammatory immune microenvironment. Blockade of the interaction between PCWBR2 and integrin α_2/β_1 abolishes *P. anaerobius*-mediated CRC in *Apc*^{Min/+} mice. Therefore, this study identifies a mechanism whereby *P. anaerobius* contributes

¹Institute of Digestive Disease and Department of Medicine and Therapeutics, The Chinese University of Hong Kong, Hong Kong SAR, China.

²State Key Laboratory of Digestive Disease, Li Ka Shing Institute of Health Sciences, The Chinese University of Hong Kong, Hong Kong SAR, China.

³Chinese University of Hong Kong–Shenzhen Research Institute, Shenzhen, China. ⁴Department of Anatomical and Cellular Pathology, The Chinese University of Hong Kong, Hong Kong SAR, China. *e-mail: junyu@cuhk.edu.hk

to CRC and establishes a PCWBR2-integrin α_2/β_1 interaction as a potential druggable target in CRC.

Results

***P. anaerobius* accelerates colorectal tumorigenesis in *Apc*^{Min/+} mice.** To test the effect of *P. anaerobius* on colorectal tumorigenesis, we used *Apc*^{Min/+} mice, a genetic mice model of spontaneous CRC (Supplementary Fig. 1a). After microbiota depletion with antibiotics for 2 weeks, we gavaged the mice with 1×10^8 colony-forming units (c.f.u.) of *P. anaerobius* daily for 10 weeks. Two other mice groups (negative controls) received non-tumorigenic intestinal microflora *Escherichia coli* (*E. coli*) strain MG1655 (1×10^8 c.f.u.) or PBS, while one group of mice was gavaged with *F. nucleatum* (1×10^8 c.f.u.) as the positive control. Quantitative PCR (qPCR) confirmed that *P. anaerobius* colonized colonic tissues after inoculation (Supplementary Fig. 1b). Tumour multiplicity and weight in the colon were examined after 10 weeks of treatment. Representative images of the colon from each group are shown in Supplementary Fig. 1c. *P. anaerobius*-treated *Apc*^{Min/+} mice developed significantly higher tumour multiplicities ($P=0.0015$) and tumour weight ($P=0.003$) compared with *Apc*^{Min/+} mice treated with *E. coli* MG1655 or PBS (Fig. 1a). *F. nucleatum*, as expected, promoted CRC development; there was no significant difference between the effect of *P. anaerobius* and *F. nucleatum*. All colonic tumours were confirmed histologically (Fig. 1b). *P. anaerobius*-treated *Apc*^{Min/+} mice also demonstrated significantly higher incidence of dysplasia (63.6% high-grade dysplasia (HGD)) compared with *Apc*^{Min/+} mice treated with *E. coli* MG1655 (0% HGD) or PBS (12.5% HGD) (Fig. 1c). *P. anaerobius* also increased tumour size ($P=0.0034$) in the small intestine of *Apc*^{Min/+} mice compared with the *E. coli* MG1655 or PBS groups (Supplementary Fig. 1d). Our results suggest that *P. anaerobius* accelerates colorectal tumorigenesis in *Apc*^{Min/+} mice.

***P. anaerobius* is localized and enriched in the colonic tumour tissues of *Apc*^{Min/+} mice.** Given that *P. anaerobius* was enriched in the tissue biopsies⁶ and promoted CRC tumorigenesis in *Apc*^{Min/+} mice, we postulated that *P. anaerobius* could be localized within the tumour or its microenvironment. To examine the tissue localization of *P. anaerobius*, we performed fluorescence in situ hybridization (FISH) using *P. anaerobius* oligonucleotide probes on colonic tumours and adjacent normal tissues from *Apc*^{Min/+} mice. As shown in Fig. 1d, *P. anaerobius* was enriched in colonic tumours compared to adjacent normal tissue sections. Regions for colonic tumour and adjacent normal tissues were confirmed histologically (Supplementary Fig. 1e). In addition, qPCR analyses confirmed increased *P. anaerobius* levels in colonic tumours from *Apc*^{Min/+} mice compared to adjacent normal tissues in the *P. anaerobius*-treated group ($P=0.0098$) (Fig. 1e). Our data indicate that *P. anaerobius* is localized and enriched in the colonic tumour tissues of *Apc*^{Min/+} mice.

***P. anaerobius* attaches preferentially to CRC cell lines.** Since we demonstrated that *P. anaerobius* colonizes colonic tumours in *Apc*^{Min/+} mice, we next investigated the adhesion properties of *P. anaerobius* in vitro using two CRC cell lines (HT-29 and Caco-2) and one normal colon mucosal epithelial cell line (NCM460). The bacterial attachment assay revealed that *P. anaerobius* attached to all three cell lines; however, it demonstrated significantly increased attachment to both CRC cell lines compared to NCM460 cells (Fig. 2a). In contrast, non-tumorigenic *E. coli* MG1655 did not significantly attach to CRC or NCM460 cells (Fig. 2a). Next, we performed transmission electron microscopy (TEM) to visualize *P. anaerobius* attachment. The TEM images confirmed that *P. anaerobius* attaches to all three colon cell lines (Fig. 2b). *E. coli* MG1655, as the negative control, showed no attachment in all three cell lines (Fig. 2b). Moreover, live imaging of fluorescently labelled *P. anaerobius* confirmed direct attachment to Caco-2 cells (Supplementary Video 1).

These data suggest that *P. anaerobius* may exert its oncogenic effect through direct interaction with colonic epithelial cells, particularly in transformed cell lines.

The *P. anaerobius* surface protein PCWBR2 binds to integrin α_2/β_1 on CRC cells. Since *P. anaerobius* attaches preferentially to CRC cell lines, identification of the surface proteins capable of binding to host cell receptors is critical for understanding the pathogenesis of *P. anaerobius*. Using the biotin far-western method (Supplementary Fig. 2), we identified eight candidate proteins from *P. anaerobius* that interacted with biotinylated surface proteins isolated from HT-29 cells (Fig. 2c). The corresponding bands were then submitted for protein identification and characterization by mass spectrometry (Supplementary Table 1.1). Among the identified proteins, PCWBR2 was the only *P. anaerobius* surface protein (Fig. 2d). PCWBR2 consists of 762 amino acid residues with a predicted molecular mass of 81.6 kDa. No proteins with significant sequence similarity were found in *E. coli* and *F. nucleatum* by protein-protein basic local alignment search tool. To validate the binding of *P. anaerobius* PCWBR2 protein to HT-29 and Caco-2 surface membrane proteins, we pulled down *P. anaerobius* surface proteins interacting with biotinylated HT-29 and Caco-2 cell surface proteins using a biotin pull-down assay and confirmed their identity by mass spectrometry (Supplementary Table 1.2). As shown in Fig. 2e, PCWBR2 was identified as a major binding protein. Collectively, these results indicate that PCWBR2 might bind to surface receptors in HT-29 and Caco-2 cells.

Next, we sought to identify the corresponding cell surface receptors for PCWBR2 on HT-29 cells. Thus, we overexpressed recombinant glutathione S-transferase (GST)-tagged PCWBR2 in *E. coli* and performed a GST pull-down assay with HT-29 membrane proteins. Silver staining and mass spectrometry identified 16 candidate proteins that interact with GST-PCWBR2. Among these (Supplementary Table 2.1), two membrane proteins were identified as integrin α_2 (band 1) and β_1 (band 3) (Fig. 3a and Supplementary Table 2.2). Apart from integrin α_2/β_1 , anoctamin-1 is another surface membrane protein that interacts with PCWBR2 and is associated with CRC. However, validation work revealed that *P. anaerobius* did not promote the expression of anoctamin-1 after 4 h coinubation (Supplementary Fig. 3a). To validate the interaction between PCWBR2 and integrin α_2/β_1 , the GST pull-down assay was conducted in four colon cell lines—NCM460, HT-29, Caco-2 and SW48. Western blot analysis demonstrated that both integrin α_2 and β_1 were pulled down by PCWBR2 specifically (Fig. 3b). Finally, the GST pull-down assay using purified integrin α_2 and β_1 proteins confirmed their direct interactions with PCWBR2 (Fig. 3c). Integrin α_2 and β_1 are overexpressed in CRC cells (HT-29, Caco-2 and SW48) compared to the normal colonic cell line NCM460 (Supplementary Fig. 3b). Our results collectively indicate that the *P. anaerobius* surface protein PCWBR2 can directly interact with colonic cells via integrin α_2/β_1 , particularly in CRC cells overexpressing these receptor proteins.

***P. anaerobius* attaches to CRC cells via integrin α_2/β_1 through PCWBR2.** Next, we investigated the functional role of the PCWBR2-integrin α_2/β_1 interaction in CRC cells. Since bacterial attachment is essential for colonization of the colonic epithelium, we first asked whether *P. anaerobius* attachment is dependent on the interaction between PCWBR2 and integrin α_2/β_1 . To examine whether *P. anaerobius* attachment in colonic cell lines is dependent on the binding between PCWBR2 and integrin α_2/β_1 , bacterial attachment assays were conducted in four colonic cell lines (HT-29, Caco-2, SW48 and NCM460) with the integrin inhibitor RGDS peptide. In all four cell lines, RGDS suppressed *P. anaerobius* attachment in a dose-dependent manner (Fig. 3d and Supplementary Fig. 4a). Consistent with these findings, small interfering RNA mediated

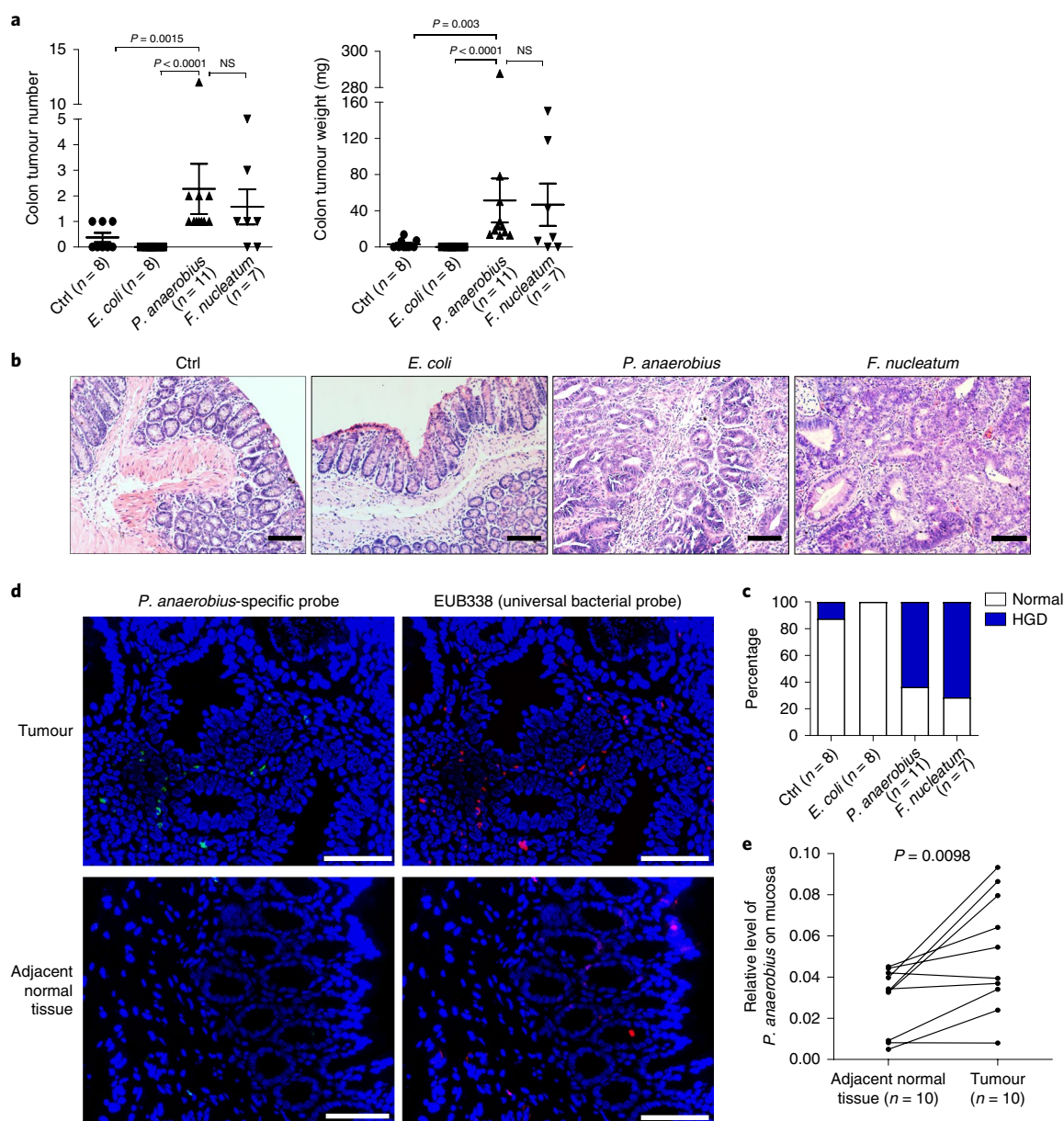


Fig. 1 | *P. anaerobius* promotes colonic tumorigenesis in *Apc^{Min/+}* mice. **a**, Colonic tumour number and tumour weight of *Apc^{Min/+}* mice were measured under different treatments. Data are presented as the mean \pm s.e.m. Statistical significance was determined by two-tailed Mann-Whitney *U*-test. NS, not significant. **b**, Representative histological images of colon tissues of *Apc^{Min/+}* mice by H&E staining. Scale bars, 100 μ m. One slide per mouse was stained with H&E. **c**, Statistical analysis of colon samples according to histological score. **d**, FISH detection of *P. anaerobius* in colonic tumours and adjacent normal tissues using a Cy3-conjugated universal bacterial 16S rDNA-directed oligonucleotide probe (EUB338, red) and Alexa Fluor 488-conjugated *P. anaerobius* specific probe (green). Scale bars, 50 μ m. Two independent experiments were performed with consistent results. **e**, *P. anaerobius* was enriched in colonic tumours ($n=10$) compared with adjacent normal tissues ($n=10$) in *Apc^{Min/+}* mice treated with *P. anaerobius*, as determined by qPCR. *P. anaerobius* levels were normalized to the *Actb* gene. The *P* value was calculated by two-tailed paired *t*-test.

the knockdown of integrin α_2 and β_1 in HT-29, Caco-2, SW48 and NCM460 cells (Fig. 3f) and reduced *P. anaerobius* attachment (Fig. 3e and Supplementary Fig. 4b). Blocking integrin α_2 and β_1 with antibodies also reduced *P. anaerobius* attachment to these cell lines (Fig. 3g and Supplementary Fig. 4c). Together, these results indicate that PCWBR2 mediates *P. anaerobius* attachment via integrin α_2/β_1 .

***P. anaerobius* promotes PI3K-Akt-NF- κ B signalling through PCWBR2-integrin α_2/β_1 interaction.** *P. anaerobius* increased cell proliferation in HT-29, Caco-2 and SW48 cell lines (Supplementary Fig. 5a). To probe the signalling events downstream of integrin α_2/β_1 ,

we performed gene expression profiling of the HT-29 and Caco-2 cell lines co-cultured with *P. anaerobius*. The gene expression profiles of HT-29 and Caco-2 cells after bacterial treatment are shown in Supplementary Tables 3.1 and 3.2, respectively. RNA sequencing (RNA-seq) revealed that 244 genes ($q < 0.25$) were consistently upregulated in both cell lines following *P. anaerobius* co-culture (Supplementary Table 3.3). Among the upregulated genes, *Itga2* and *Itgb1* were identified, further underlining their potential role in the tumour-promoting effect of *P. anaerobius*. Gene set enrichment analysis (Supplementary Fig. 5b) revealed that *P. anaerobius*-mediated gene expression was associated with the reactive oxygen

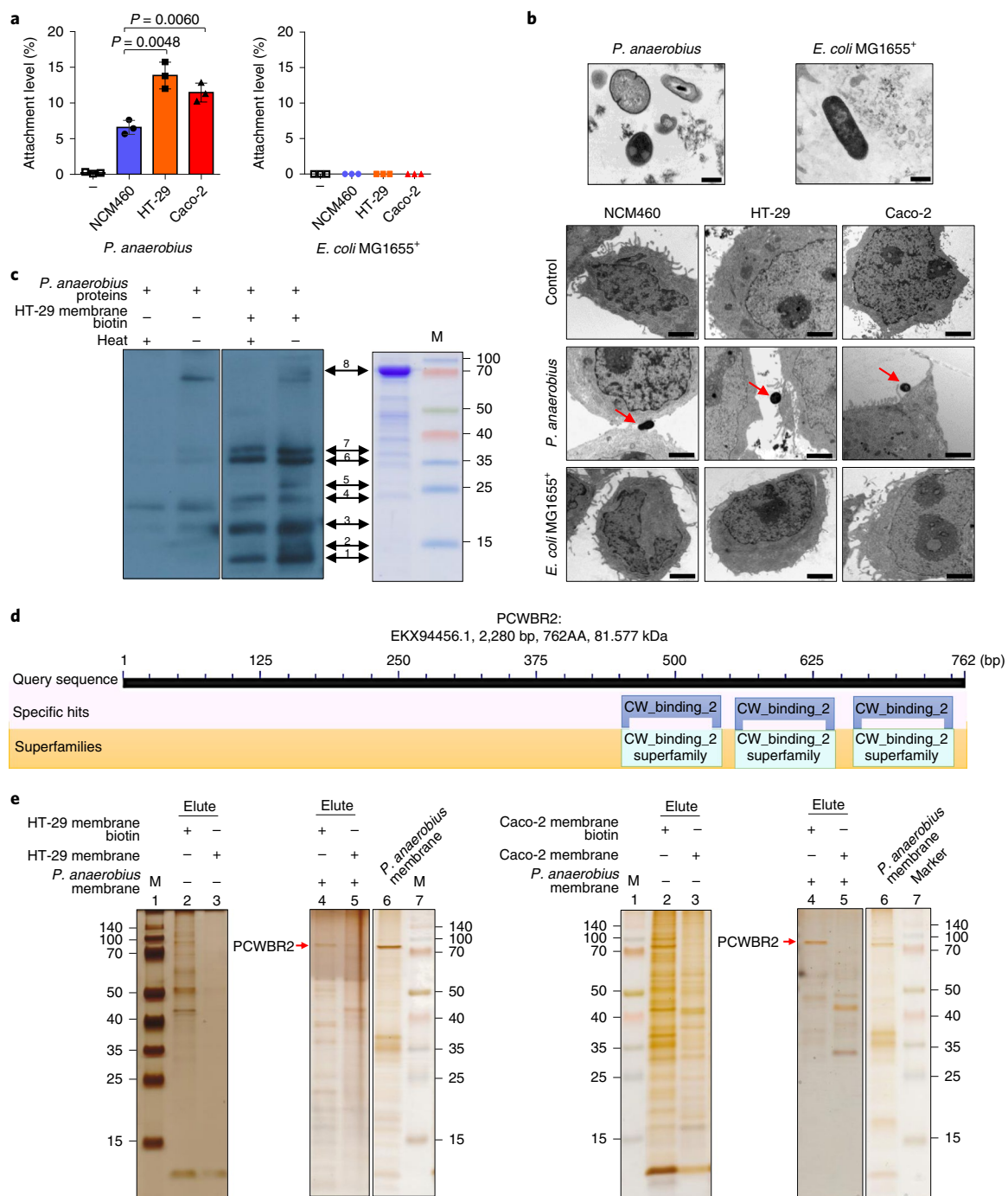


Fig. 2 | *P. anaerobius* attaches to colon cells through its surface protein PCWBR2. **a**, The level of attachment of *P. anaerobius* on colon cancer cell lines HT-29 and Caco-2 and the normal colon cell line NCM460 (MOI=10 for 1h). *E. coli* (MG1655) was used as the negative control. Data are presented as mean \pm s.d. of three biological replicates. *P* values were calculated using a two-tailed unpaired Student's *t*-test. **b**, Representative TEM images of *P. anaerobius* attaching to colon cancer HT-29 and Caco-2 cells and normal colon cells (NCM460). *E. coli* (MG1655) was used as the negative control. The red arrows indicate *P. anaerobius*. Scale bars, 500 nm in *P. anaerobius* and *E. coli* (MG1655) (upper two panels); 2 μ m for the remaining panels. **c**, Screening of *P. anaerobius* adhesins by biotin far-western assay. Immobilized whole-cell *P. anaerobius* proteins (heated and nonheated) were first incubated with or without biotinylated HT-29 membrane proteins, followed by incubation with streptavidin-HRP conjugate. Eight candidate proteins from *P. anaerobius* interacting with biotinylated surface proteins isolated from HT-29 cells were visualized on the western blots (left-hand side) and their corresponding bands from SDS-PAGE (right-hand side) were submitted for protein identification by mass spectrometry. M, marker. **d**, Sequence information of PCWBR2, the potential candidate protein of *P. anaerobius* adhesin. **e**, PCWBR2 can be pulled down by the biotin pull-down assay of the HT-29 and Caco-2 surface proteins. Biotinylated HT-29 and Caco-2 surface proteins (lanes 2 and 4, respectively) or nonbiotinylated HT-29 and Caco-2 surface proteins (lanes 3 and 5, respectively) were first incubated with streptavidin agarose resin, followed by incubation with (lanes 4 and 5) or without (lanes 2 and 3) *P. anaerobius* surface membrane proteins (lane 6). Eluted proteins were subjected to SDS-PAGE and visualized by silver staining. Lanes 1 and 7 contained the marker. The left- and right-hand panels show the biotin pull-down assay for HT-29 and Caco-2 cells, respectively. Two independent experiments were performed with similar results, as in **b, c, e**.

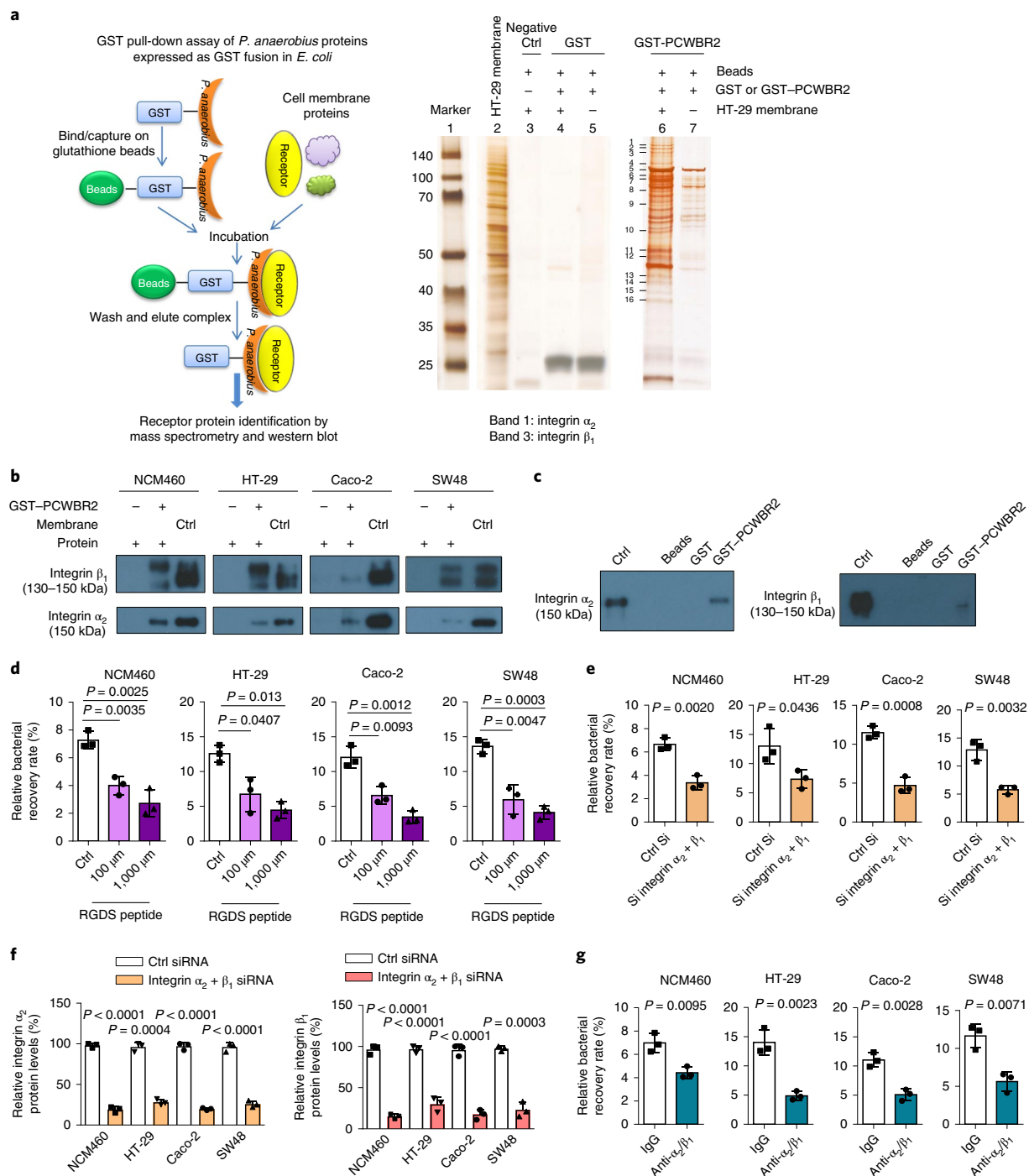


Fig. 3 | *P. anaerobius* attaches to colon cells by interacting with the epithelial cell surface receptor integrin α_2/β_1 . **a**, PCWBR2 is overexpressed in the GST fusion system to pull down its corresponding receptors on the host cell line. GST agarose beads were first incubated with GST (lanes 4 and 5) and GST-PCWBR2 (lanes 6 and 7) separately, followed by incubation with (lanes 4 and 6) or without (lanes 5 and 7) HT-29 membrane proteins overnight at 4 °C. The beads were then washed and boiled with SDS-PAGE gel loading buffer. Eluted proteins were separated by SDS-PAGE and analysed by silver staining or western blot. HT-29 membrane proteins were used to show the protein bands in the silver staining gels (lane 2). For the negative control, only beads were incubated with the HT-29 membrane proteins (lane 3). Silver staining and mass spectrometry showed 16 candidate proteins that interact with GST-PCWBR2. Among the identified proteins, two membrane proteins were identified as integrin α_2 (band 1) and β_1 (band 3). Lane 1 contained the marker. **b**, GST pull-down assays were performed to validate the interaction of GST-PCWBR2 with integrin α_2/β_1 in NCM460, HT-29, Caco-2 and SW48 cells lines by western blot. Ctrl, membrane proteins isolated from these four cell lines. **c**, GST pull-down assays were performed with purified, commercially available recombinant integrin α_2 and β_1 . **d**, The integrin inhibitor RGDS peptide suppressed *P. anaerobius* attachment in the NCM460, HT-29, Caco-2 and SW48 cells lines (100 μ M and 1,000 μ M RGDS peptides were used). **e**, Silencing of integrin α_2 and β_1 suppressed *P. anaerobius* attachment in NCM460, HT-29, Caco-2 and SW48 cells lines. **f**, Knockdown efficiency of integrin α_2 and β_1 siRNA in NCM460, HT-29, Caco-2 and SW48 cells. **g**, Antibody blocking of integrin α_2/β_1 suppressed *P. anaerobius* attachment in NCM460, HT-29, Caco-2 and SW48 cells; 10 μ g ml⁻¹ antibody or isotype control were used. **d–g**, Data are presented as the mean \pm s.d. *P* values were determined by two-tailed unpaired Student's *t*-test. Three independent experiments were performed with consistent results.

species pathway, apical junction pathway, PI3K–Akt–mTOR signalling and cholesterol homeostasis. Integrins are key components of the apical junction pathway by inducing focal adhesion kinase (FAK) phosphorylation, which in turn phosphorylates the p85 subunit of PI3K (refs. 18,19). Thus, we hypothesized that *P. anaerobius* activates the PI3K–Akt pathway via PCWBR2–integrin α_2/β_1 to promote tumorigenesis. To test this, we examined the messenger RNA expression of genes involved in the PI3K–Akt cascade and found significant upregulation of key PI3K–Akt pathway genes including *Itga2*, *Itgb1*, *Pik3r1*, *Akt1* and *Nfkb1* in HT-29, Caco-2 and SW48 cells treated with *P. anaerobius* (Supplementary Fig. 5c). Accordingly, *P. anaerobius* increased protein expression of integrin α_2/β_1 , FAK, phospho-FAK (p-FAK), PI3K (p85), p-PI3K (p85), Akt, p-Akt, NF- κ B p65 (RelA) and p-p65 as determined by western blot (Fig. 4a and Supplementary Fig. 6a). Proliferating cell nuclear antigen (PCNA), a cell proliferation marker, was also induced by *P. anaerobius*. Co-treatment with the integrin inhibitor RGDS peptide (Fig. 4a and Supplementary Fig. 6a), integrin α_2/β_1 small interfering RNA (Fig. 4b and Supplementary Fig. 6b) or integrin α_2/β_1 antibodies (Fig. 4c and Supplementary Fig. 6c) abrogated the *P. anaerobius*-induced integrin α_2/β_1 –PI3K–Akt–p65 signalling cascade and PCNA protein expression. Moreover, there was no activation of the integrin α_2/β_1 –PI3K/Akt/NF- κ B signalling cascade in normal colon NCM460 cells after *P. anaerobius* treatment (Supplementary Fig. 7). Our findings suggest that *P. anaerobius* promotes PI3K–Akt–NF- κ B signalling through PCWBR2–integrin α_2/β_1 interaction.

***P. anaerobius* activates the integrin α_2/β_1 –PI3K–Akt–NF- κ B signalling cascade in *Apc*^{Min/+} mice.** Next, we sought to validate the effect of *P. anaerobius* on signalling cascades in *Apc*^{Min/+} mice. qPCR analyses of colonic tumours from *Apc*^{Min/+} mice treated with vehicle or *P. anaerobius* revealed significant upregulation of *Itga2* ($P=0.0416$), *Itgb1* ($P=0.0396$), *Akt1* ($P=0.0223$) and *Nfkb1* ($P=0.0386$) in *P. anaerobius*-treated tumours (Fig. 4d). In addition, protein expression of integrin α_2 ($P=0.0057$), integrin β_1 ($P=0.0282$), PI3K (p85) ($P=0.0099$), p-PI3K ($P=0.0140$) Akt ($P=0.0362$), p-Akt ($P=0.0014$), NF- κ B p65 ($P=0.0456$) and p-NF- κ B p65 ($P=0.0354$) were all upregulated in the tumours of *P. anaerobius*-treated *Apc*^{Min/+} mice (Fig. 4e and Supplementary Fig. 8). Activation of these signalling cascades is consequential, with *P. anaerobius*-treated *Apc*^{Min/+} tumours showing increased cell proliferation, as evidenced by higher PCNA protein expression (Fig. 4e and Supplementary Fig. 8) and Ki-67⁺ cells (Fig. 4f) compared to tumours from the vehicle-treated group. These results are largely in line with in vitro observations, thereby confirming that *P. anaerobius* activates the integrin α_2/β_1 –PI3K–Akt–NF- κ B signalling cascade in vivo.

***P. anaerobius* increases the expression of pro-inflammatory cytokines in *Apc*^{Min/+} mice.** We investigated the molecular mechanisms of *P. anaerobius* in inducing colonic tumorigenesis. We performed a PCR array to profile the expression of 84 key genes involved in the inflammatory response and autoimmunity in colonic tumours from *P. anaerobius*-treated and control *Apc*^{Min/+} mice. *P. anaerobius* upregulated the majority of inflammation-related genes (60) by >1.5-fold, while only 2 genes were downregulated (Fig. 5a and Supplementary Table 4). We observed robust upregulation of immune marker genes associated with myeloid-derived suppressor cells (MDSCs) (*Il10*, *Ifng*, *Csf1*, *Il6*, *Ptgs2* and *Nfkb1*), tumour-associated macrophages (TAMs) (*Ccl17*, *Ccl22*, *Il1r1*, *Il1a*, *Cxcl10* and *Tnf*) and tumour-associated neutrophils (TANs) (*Cxcl1*, *Cxcl2*, *Cxcl5*, *Tnf* and *Il17a*) (Supplementary Table 4) in colonic tumours from *P. anaerobius*-treated *Apc*^{Min/+} mice. qPCR (Fig. 5b and Supplementary Fig. 9a), confirmed upregulation of cytokines such as *Il10* ($P=0.0274$), *Ifng* ($P=0.0136$) (Fig. 5b) and *Nfkb1* ($P=0.0386$) (Fig. 4d). Taken together, our data indicate that *P. anaerobius* can induce a

pro-inflammatory response in CRC associated with the enrichment of specific tumour-infiltrating immune cell populations.

***P. anaerobius* modifies the tumour immune microenvironment to promote CRC.** To directly address the effect of *P. anaerobius* on the tumour immune landscape in CRC, we analysed the composition of tumour-infiltrating immune cells isolated from the colon of *Apc*^{Min/+} mice using multicolour flow cytometry (Fig. 5c and Supplementary Fig. 9b). Consistent with the qPCR results, we observed highly significant enrichment of MDSCs ($P=0.0003$), TAMs ($P=0.0402$) and granulocytic TANs (GTANs; $P=0.0210$) in *Apc*^{Min/+} mice treated with *P. anaerobius* compared to *Apc*^{Min/+} mice treated with control PBS (Fig. 5c). MDSCs are tumour-permissive myeloid cells with immune suppressive activity²⁰. We further analysed two subsets of MDSCs, monocytic MDSCs (M-MDSCs) and granulocytic MDSCs (G-MDSCs); both were increased in *P. anaerobius*-treated mice compared to controls (Fig. 5c). M-MDSCs mainly generate nitric oxide and can be precursors of TAMs²¹, whereas G-MDSCs produce reactive oxygen species and can differentiate into GTANs²². Thus, we analysed TAMs, including M₂-like TAMs and GTANs; the results showed that both TAMs and GTANs were enriched the *P. anaerobius*-treated mice compared to controls (Fig. 5c). There were no significant differences in the three subtypes of dendritic cells after *P. anaerobius* treatment. Tumour-infiltrating cytotoxic T cells were slightly increased ($P=0.0098$) in *P. anaerobius*-treated *Apc*^{Min/+} mice (Fig. 5c). We also observed that regulatory T (Treg) cells and T helper 17 (T_H17) cells were increased in *P. anaerobius*-treated *Apc*^{Min/+} mice compared to controls (Supplementary Fig. 9c,d). Treg and T_H17 cells are highly associated with intestinal inflammation and CRC²³ and levels of IL-23 and IL-10, both of which were upregulated in *P. anaerobius*-treated *Apc*^{Min/+} mice (Fig. 5a). Inflammation-driven cancers are characterized by increased T_H17 infiltration and reduced Treg cells. The unexpected upregulation of Treg cells may have arisen because we used the whole colon for flow cytometry analysis. Collectively, our results suggest that *P. anaerobius* affects numerous types of immune cells, especially the immune-suppressive MDSCs, TAMs and GTANs, to promote tumour progression.

Blockade of integrin α_2/β_1 attenuates the pro-tumorigenic and signalling effect of *P. anaerobius* in *Apc*^{Min/+} mice. To verify the role of PCWBR2–integrin α_2/β_1 interaction in the pro-tumorigenic effect of *P. anaerobius* in *Apc*^{Min/+} mice, we blocked integrin α_2/β_1 by injecting mice intraperitoneally with RGDS peptide (200 μ g per mouse, three times a week for 10 weeks) (Supplementary Fig. 10a). Representative images of the colon from each group are shown in Supplementary Fig. 10b. RGDS peptide significantly decreased colonic tumour number ($P=0.0109$) and weight ($P=0.0171$) in *Apc*^{Min/+} mice treated with *P. anaerobius* (Fig. 6a). RGDS peptide had no effect on control *Apc*^{Min/+} mice, suggesting that integrin α_2/β_1 does not promote tumorigenesis in the absence of *P. anaerobius*. The PI3K–Akt pathway genes upregulated by *P. anaerobius* in *Apc*^{Min/+} mice, including *Itga2* ($P=0.0305$), *Itgb1* ($P=0.0176$), *Akt1* ($P=0.0090$) and *Nfkb1* ($P=0.0273$), were abrogated by RGDS peptide treatment (Fig. 6b). In addition, protein expression of integrin α_2 ($P=0.0275$), integrin β_1 ($P=0.0268$), PI3K (p85) ($P=0.0463$), p-PI3K ($P=0.0342$), Akt ($P=0.0415$), p-Akt ($P=0.0376$), NF- κ B p65 ($P=0.0444$), p-NF- κ B p65 ($P=0.0498$) and PCNA ($P=0.0491$) were downregulated by RGDS peptide in the tumours of *P. anaerobius*-treated *Apc*^{Min/+} mice (Fig. 6c). RGDS peptide treatment reversed the effect of *P. anaerobius* on cell proliferation (Ki-67) in *Apc*^{Min/+} tumours (Fig. 6d). Apart from tumour-intrinsic response, RGDS peptide attenuated the level of *P. anaerobius*-associated pro-inflammatory factors such as *Nfkb1* ($P=0.0273$) (Fig. 6b), *Il10* ($P=0.0171$) and *Ifng* ($P=0.0449$) (Fig. 6e). To confirm the role of inflammation in *P. anaerobius*-promoted colonic tumorigenesis, mice were treated with the cyclooxygenase-2 inhibitor celecoxib (Supplementary Fig. 11a,b).

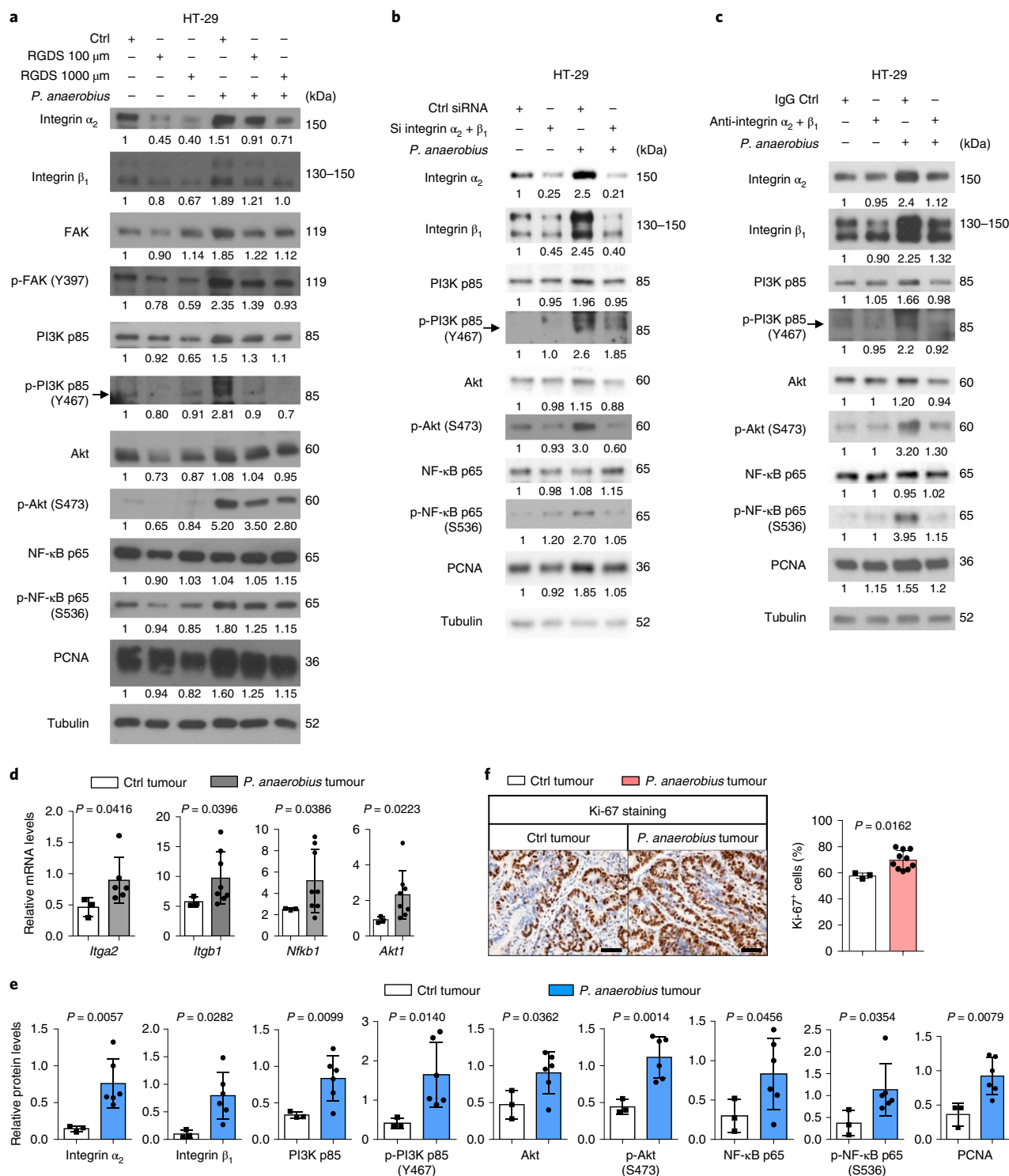


Fig. 4 | *P. anaerobius* mediates integrin β_1/α_2 signalling to activate the PI3K-Akt pathway to promote cell proliferation in vitro, and these effects are verified in *Apc*^{Min/+} mouse model. **a, Validation of integrin α_2/β_1 -PI3K-Akt-NF- κ B signalling pathway and cell proliferation triggered by *P. anaerobius* by western blot in HT-29 cells. The effects of *P. anaerobius* were abolished by the integrin inhibitor RGDS peptide (100 μ M and 1,000 μ M) in a dose-dependent manner. **b**, Integrin α_2/β_1 knockdown abolished the effect of *P. anaerobius* on the α_2/β_1 -PI3K-Akt-NF- κ B pathway and cell proliferation in HT-29 cell lines. **c**, Antibody blocking of integrin α_2/β_1 suppressed the effect of *P. anaerobius* on the α_2/β_1 -PI3K-Akt-NF- κ B pathway and cell proliferation in HT-29 cell lines. Tubulin was used as the loading control. Band intensity was measured with ImageJ and the ratio of each band was normalized to the corresponding tubulin and is shown below each band. Three independent experiments were repeated with similar results in **a-c**. **d**, qPCR was performed in mouse colon tumour tissues to validate a subset of key integrin α_2/β_1 -PI3K-Akt-NF- κ B pathway genes in colon cancer cells. **e**, Quantitative analysis of altered protein expression of key integrin α_2/β_1 -PI3K-Akt-NF- κ B pathway proteins by western blot (Supplementary Fig. 8). **f**, Immunohistochemistry showing Ki-67⁺ cells in colon tumours of *Apc*^{Min/+} mice after vehicle and *P. anaerobius* gavage and quantitative analysis. Scale bars, 50 μ m. Three colon tumour tissues from the vehicle-treated group and 6–10 colon tumour tissues from the *P. anaerobius*-treated groups were used in **d-f**. Data are presented as the mean \pm s.d. in **d-f**. **d-f**, P values were determined by two-tailed unpaired Student's t -test.**

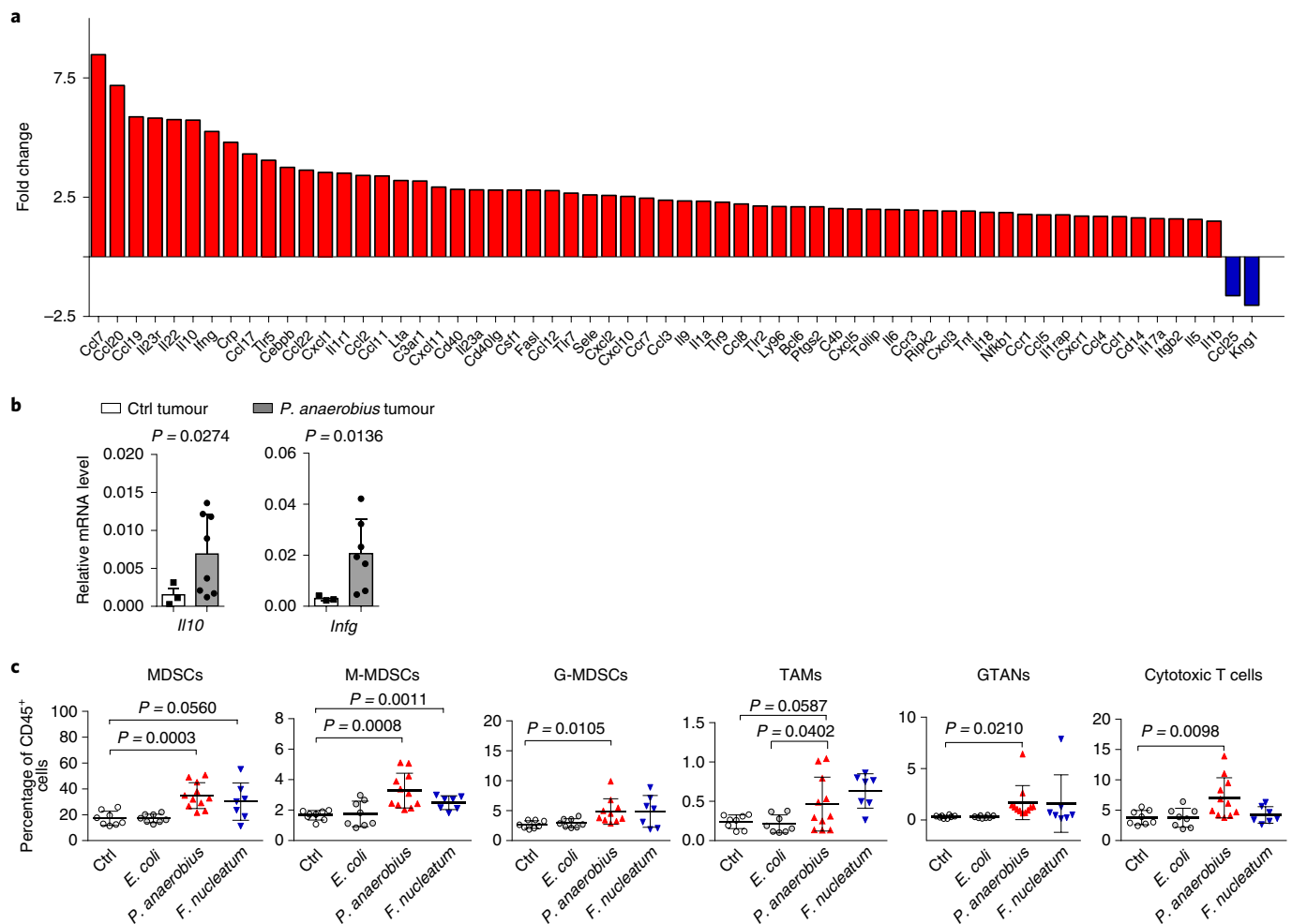


Fig. 5 | *P. anaerobius* modifies the tumour immune microenvironment to promote CRC. **a**, The upregulation of 60 genes (red) and downregulation of 2 genes (blue) were identified by mouse inflammatory response and autoimmunity PCR array using colon tumour tissues from *P. anaerobius*- versus vehicle-treated *Apc*^{Min/+} mice. The fold change of selected cytokines, chemokines and pro-inflammatory factors related to MDSCs (*Il10*, *Infg*, *Csf1*, *Il6*, *ptgs2* and *Nfkb1*), TAMs (*Ccl17*, *Ccl22*, *Il1r1*, *Il1a*, *Cxcl10* and *Tnf*) and TANs (*Cxcl1*, *Cxcl2*, *Cxcl5*, *Tnf* and *Il17a*) is shown. A single experiment was performed. **b**, qPCR validation of selected cytokine genes in colon tumours from *P. anaerobius*- versus vehicle-treated *Apc*^{Min/+} mice. Two or three colon tumour tissues from the vehicle-treated group and 6–9 colon tumour tissues from the *P. anaerobius*-treated group were used. Data are presented as mean \pm s.d. *P* values were determined by two-tailed unpaired Student's *t*-test. **c**, *P. anaerobius* contributes to CRC tumorigenesis by expanding MDSCs, TAMs and GTANs. Profiling of tumour-infiltrating immune cells isolated from the *Apc*^{Min/+} mice colon by multicolour flow cytometry, including MDSCs, M-MDSCs, G-MDSCs, TAMs, GTANs and cytotoxic T cells; 7–11 mice were used in each group (Ctrl group, *n* = 8; *E. coli* (MG1655) group, *n* = 8; *P. anaerobius* group, *n* = 11; *F. nucleatum* group, *n* = 7). Data are presented as the mean \pm s.d. *P* values were determined by two-tailed unpaired Student's *t*-test.

As expected, celecoxib significantly reduced the colonic tumour number ($P = 0.007$) and weight ($P = 0.0175$) induced by *P. anaerobius* in *Apc*^{Min/+} mice (Supplementary Fig. 11c). Collectively, our findings validate the underlying role of the integrin α_2/β_1 -PI3K-Akt-NF- κ B signalling cascade in *P. anaerobius*-mediated colorectal tumorigenesis in *Apc*^{Min/+} mice.

Discussion

Increasing evidence indicates that microbial dysbiosis contributes to CRC development²⁴. Metagenomic profiling of stool and mucosal samples from CRC patients^{5,6} revealed that *P. anaerobius* is an oncogenic bacterial candidate enriched in CRC. However, whether and how *P. anaerobius* may promote colorectal tumorigenesis remains unknown. In this study, we demonstrated the oncogenic potential of *P. anaerobius* in mice and elucidated a mechanism by which *P. anaerobius* communicates with colonic epithelial cells to promote cell proliferation and modulate the immune microenvironment.

In microbiota-depleted *Apc*^{Min/+} mice, *P. anaerobius* significantly promotes colorectal tumorigenesis with regard to both tumour multiplicity and size. *P. anaerobius* accumulates specifically in the tumorous regions of the colon in *Apc*^{Min/+} mice, suggesting that it might interact with CRC cells. Consistent with in vivo observations, we show that *P. anaerobius* avidly adheres to colonic epithelial cells in vitro, with a stronger affinity for CRC cell lines compared to normal colonic cells. Bacterial adherence and colonization are often prerequisite steps to tumour promotion, as in the case of *F. nucleatum*¹³ and *B. fragilis*¹¹. These findings encouraged us to further explore the molecular basis of the *P. anaerobius*-CRC cellular interaction.

Using a biotin far-western blot approach, we identified a *P. anaerobius* surface protein, PCWBR2, which directly interacts with cell surface epithelial receptors on CRC cells. Reciprocal immunoprecipitation demonstrated that PCWBR2 functions as a ligand for the integrin α_2/β_1 receptor expressed on colonic cells. Adherence

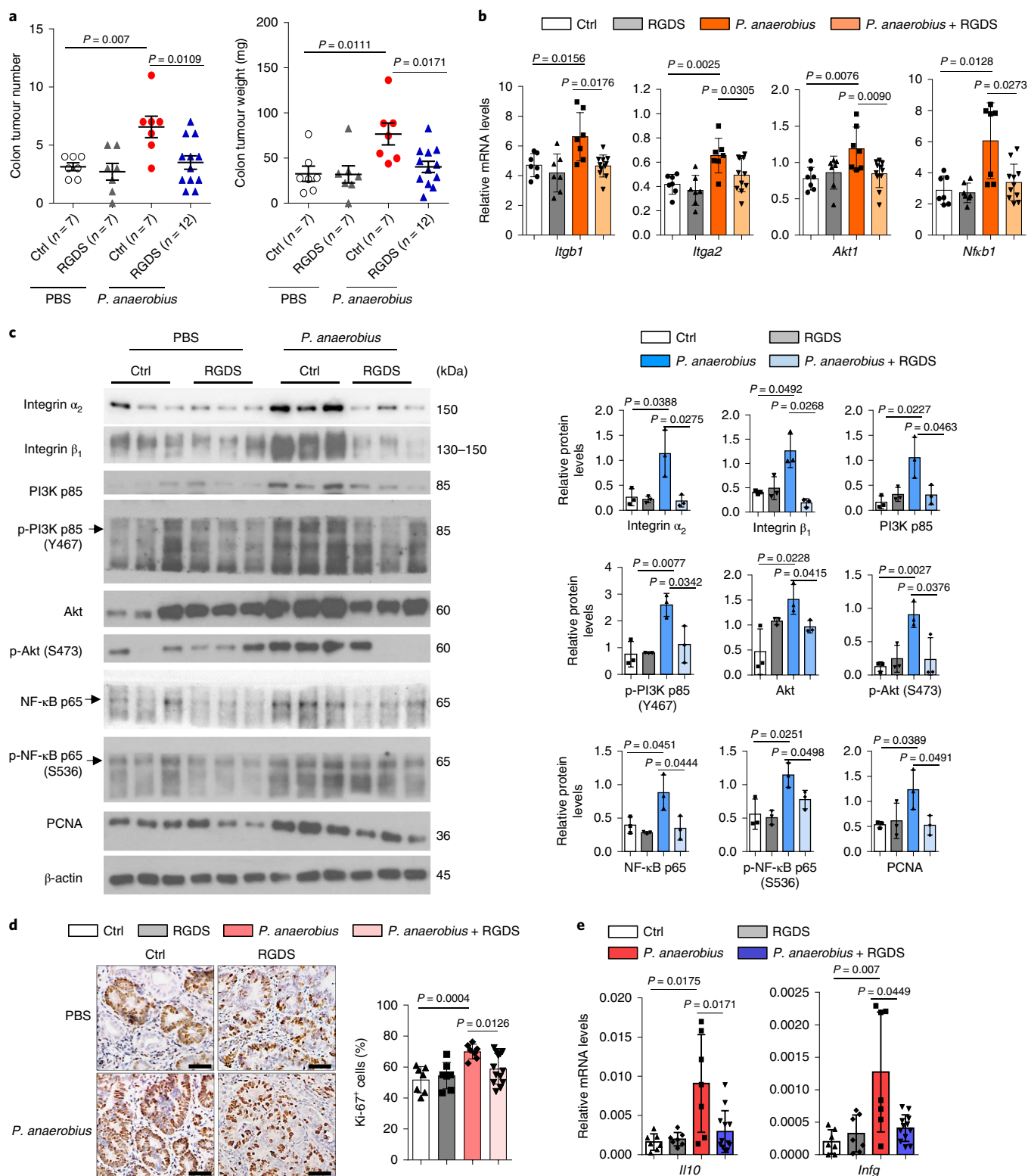


Fig. 6 | Blockade of integrin β_1/α_2 -attenuated *P. anaerobius*-associated colon tumorigenesis in *Apc^{Min/+}* mice. **a, For the blockade experiments, four groups of *Apc^{Min/+}* mice were included: (1) Ctrl ($n = 7$); (2) RGDS peptide ($n = 7$); (3) *P. anaerobius* ($n = 7$); and (4) *P. anaerobius* plus RGDS ($n = 12$). The colon tumour number and weight of *Apc^{Min/+}* mice in the different groups were measured. Data are presented as the mean \pm s.e.m. P values were determined by two-tailed Mann-Whitney U-test. **b**, qPCR analysis of integrin β_1/α_2 -PI3K-Akt-NF- κ B pathway genes in colon tumours. **c**, Western blot and quantitative analysis of the integrin β_1/α_2 -PI3K-Akt-NF- κ B pathway. β -actin was used as the loading control. Three mice were used from each group. **d**, Immunohistochemistry showing Ki-67⁺ cells in colon tumours. Scale bars, 50 μ m. **e**, qPCR analysis of *Il10* and *Ifng*. **a,b,d,e**, Number of mice used for each group: (1) Ctrl ($n = 7$); (2) RGDS ($n = 7$); (3) *P. anaerobius* ($n = 7$); and (4) *P. anaerobius* + RGDS ($n = 12$). **b,c,d**, Data are presented as the mean \pm s.d. **b-e**, P values were determined by two-tailed unpaired Student's t-test.**

of *P. anaerobius* to CRC cells requires PCWBR2-integrin α_2/β_1 interaction, since the integrin inhibitor RGDS peptide, knockdown of integrin α_2/β_1 and integrin α_2/β_1 -blocking antibodies abrogated *P. anaerobius* attachment in colonic cells. Integrins are surface adhesion receptors that mediate cell–cell or cell–matrix interactions¹⁴. We demonstrated that the integrin α_2/β_1 complex is overexpressed in CRC cells compared to normal colonic cells (Supplementary Fig. 3b,c), thereby contributing to increased *P. anaerobius* adherence in tumour tissues. Moreover, *P. anaerobius* stimulates the expression of integrin α_2/β_1 in CRC cells to promote adhesion in a positive regulatory circuit. Consistent with our findings, bacterial pathogens have been reported to interact with host cell integrins during their pathogenesis^{25,26}. Taken together, *P. anaerobius* interacts with host CRC cells primarily via a PCWBR2-integrin α_2/β_1 protein complex.

Engagement of integrin α_2/β_1 by *P. anaerobius* PCWBR2 is followed by the activation of an oncogenic signalling cascade in CRC cells. In *P. anaerobius*-treated CRC cells and *Apc*^{Min/+} mice, the integrin α_2/β_1 complex promotes FAK phosphorylation, which subsequently activates the PI3K–Akt signalling pathway (Supplementary Fig. 12). The PI3K–Akt pathway plays an important role in the regulation of cell survival, proliferation and apoptosis, as well as the modulation of various inflammatory responses²⁷. Correspondingly, *P. anaerobius* induces cell proliferation in both cell lines and animal CRC models. The integrin inhibitor RGDS peptide, integrin α_2/β_1 antibodies or integrin α_2/β_1 siRNA abolished *P. anaerobius*-mediated PI3K–Akt signalling and cell proliferation, supporting the notion that the PCWBR2-integrin α_2/β_1 interaction is essential for the tumour-promoting effect of this bacterium.

Beyond its effect on CRC cell proliferation, we uncovered that *P. anaerobius* provokes a pro-inflammatory immune microenvironment permissive for colorectal tumorigenesis. *P. anaerobius* broadly induced the expression of pro-inflammatory cytokines *in vivo*, which are associated with the recruitment of tumour-infiltrating MDSCs, TAMs and GTANs in the tumours of *P. anaerobius*-treated *Apc*^{Min/+} mice. Such effects are probably mediated by NF- κ B activation. MDSCs generate the immune-suppressive cytokines IL-6 and IL-10 that could directly suppress CD4⁺ and CD8⁺ T cell activities²⁸. Likewise, TAMs block the T cell antitumour response and are involved in the promotion of angiogenesis and metastasis²⁹. Modulation of the tumour immune microenvironment also underlies the tumour-promoting effect of *B. fragilis* and *F. nucleatum*, although distinct immune cell populations are induced by different bacterial species^{11,12}. Hence, pro-inflammatory stimulation and selective enrichment of immune-suppressive MDSCs/TAMs/GTANs represents an alternative mechanism by which *P. anaerobius* facilitates colorectal tumorigenesis.

In summary, we identified *P. anaerobius* as a bacterium that promotes CRC via direct interaction of its surface protein PCWBR2 with integrin α_2/β_1 , which is overexpressed on CRC cells. PCWBR2-integrin α_2/β_1 interaction promotes *P. anaerobius* adhesion and initiates an oncogenic PI3K–Akt–FAK cascade to promote tumour cell proliferation, while concomitantly reshaping the tumour immune landscape to promote tumorigenesis (Supplementary Fig. 12). Our work also shows that blockade of integrin-mediated signalling could be an effective approach to inactivate *P. anaerobius* as a preventive or treatment therapy for CRC.

Methods

Bacterial strains and culture conditions. *P. anaerobius* (27337), *F. nucleatum* (25586) and *E. coli* MG1655 (700926) were purchased from ATCC. *P. anaerobius* and *F. nucleatum* were maintained in Wilkins–Chalgren anaerobe broth (Thermo Fisher Scientific) in an anaerobic jar (80% N₂, 10% H₂, 10% CO₂) at 37°C. *E. coli* MG1655 was cultured in lysogeny broth at 37°C.

Animal experiments. Male C57BL/6 *Apc*^{Min/+} mice (6 weeks old) were administered an antibiotic cocktail in drinking water (0.2 g l⁻¹ ampicillin,

neomycin and metronidazole, and 0.1 g l⁻¹ vancomycin) for 2 weeks. One week after antibiotic treatment, mice were randomly divided into several groups and gavaged with 1 × 10⁸ c.f.u. of *P. anaerobius*, *F. nucleatum*, *E. coli* MG1655 or PBS daily for 10 weeks (Supplementary Fig. 1a). For the integrin α_2/β_1 blockade, RGDS peptide (200 µg per mouse) was given to two additional groups of mice (one group treated with PBS and the other treated with *P. anaerobius*) three times a week by intraperitoneal injection for 10 weeks (Supplementary Fig. 10a). For celecoxib treatment³⁰, celecoxib (300 ppm in the diet) was given to two additional groups of mice (one group treated with PBS and the other treated with *P. anaerobius*) for 10 weeks together with *P. anaerobius* treatment (Supplementary Fig. 11a). At the end of the experiment, mice were killed; the number and size of the small intestine, and the number and weight of colonic tumours were determined. Colonic tumours and adjacent normal tissues were collected and stored in 10% buffered formalin or snap-frozen for subsequent analysis. No statistical methods were used to predetermine sample size. The investigators were not blinded to allocation during the experiments and outcome assessment. All animal work was approved by the Animal Experimentation Ethics Committee of The Chinese University of Hong Kong.

Assessment of colonic histopathology. Paraffin-embedded colonic sections (5 µm thick) were stained with haematoxylin and eosin (H&E) and reviewed in a blinded manner by an experienced pathologist. Dysplasia was defined according to the latest World Health Organization Classification of Tumours of the Digestive System.

FISH. FISH was performed as described previously¹². A *P. anaerobius* Alexa Fluor 488-conjugated specific probe (ATGTTATCCATGTGTATAGGGC) was labelled with Spectrum-Green (Thermo Fisher Scientific). A Cy3-conjugated EUB338 universal bacterial probe (GCTGCCTCCCGTAGGAGT), as the positive control, was labelled with Spectrum-Red (Thermo Fisher Scientific). Briefly, frozen colon tissue was fixed in Carnoy's solution overnight and embedded in paraffin; 5 µm thick sections were hybridized in the hybridization buffer (0.9 M NaCl, 20 mM Tris/HCl, pH 7.3, 0.01 % SDS). Stringency was used with the formamide concentration from 0 to 30% (v/v). Pre-warmed hybridization buffer (20 ml) was mixed with approximately 5 pmol of the oligonucleotide probe and carefully applied to the tissue sections. After incubation for 5 h in a dark humid chamber at 46°C, each of the slides were rinsed with sterile double-distilled water, air-dried in the dark and mounted with ProLong Gold Antifade Mountant with DAPI (Thermo Fisher Scientific).

Microbial DNA extraction and *P. anaerobius* quantification. Mucosal tissues were digested in PBS containing an enzymatic cocktail of mutanolysin (250 U ml⁻¹) and lysozyme (1 mg ml⁻¹) (Sigma-Aldrich) at 37°C for 1 h; total genomic DNA was extracted with the QIAamp DNA Mini Kit (QIAGEN) according to the manufacturer's instructions. qPCR was performed to detect the *P. anaerobius* level by using 40 ng genomic DNA in 20 µl universal SYBR Green PCR Master Mix (Roche) on the QuantStudio 7 Flex System (Thermo Fisher Scientific). *P. anaerobius* quantitation was measured relative to the *Actb* gene. The primers used for detecting *P. anaerobius* are listed in Supplementary Table 5.

Cell culture. The colon cancer cell lines HT-29, Caco-2 and SW48 were obtained from ATCC. The normal colon immortalized epithelial cell line NCM460 was obtained from INCELL. Cell authentication was confirmed by short tandem repeat profiling. Routine *Mycoplasma* testing was performed by PCR. For bacterial co-culture, approximately 1 × 10⁵ colon cells were grown in a 24-well plate in DMEM (Thermo Fisher Scientific) supplemented with 10% FCS. Cells were exposed to *P. anaerobius* or *E. coli* MG1655 with a multiplicity of infection (MOI) of 100 for 4 h under anaerobic conditions. For inhibitor treatment, RGDS peptide (100 µM or 1,000 µM) was added 30 min before bacterial co-culture. To block integrin, anti- α_2 (P1E6) (5 µg ml⁻¹) and anti- β_1 (JB1A) (5 µg ml⁻¹) antibodies and isotype immunoglobulin G (IgG; 10 µg ml⁻¹) were added 1 h before bacterial co-culture.

Bacterial attachment assay. The bacterial attachment assay was performed as described previously³¹; 1 × 10⁵ colonic cells were grown in a 24-well plate and co-cultured with bacteria for 1 h (MOI = 10) under anaerobic conditions. After co-culture, medium was removed and cells were washed with PBS three times. To lyse the cells, 100 µl of H₂O was added for 20 min, followed by the addition of 400 µl of Wilkins–Chalgren anaerobe broth to homogenize the cells. The attached *P. anaerobius* colonies were recovered on Wilkins–Chalgren anaerobe agar plate under anaerobic conditions; the number of colonies was counted. *E. coli* MG1655 was used as the negative control.

Cell viability assay. For cell viability assay, 1 × 10⁴ colon cells were grown in a 24-well plate and co-cultured with bacteria for 2 h (MOI = 100) under anaerobic conditions. After 2 h, the medium containing the bacteria was replaced with DMEM supplemented with 10% FCS, 1% penicillin–streptomycin and 20 µg ml⁻¹ gentamycin. The co-culture was performed for four consecutive days.

3-(4,5-Dimethylthiazol-2-yl)-2,5-diphenyltetrazolium bromide (MTT) (5 mg ml⁻¹; Promega) was added to the culture (equal to one-tenth the original culture volume). After 4 h incubation at 37 °C, 400 µl of a solution containing 10% SDS and 0.01 N HCl was added. Absorbance at 570 nm was measured on a microplate reader.

Live imaging of fluorescence-labelled *P. anaerobius*. *P. anaerobius* was labelled with Click-iT Alexa Fluor 488 sDIBO (Thermo Fisher Scientific) as described previously³². Briefly, *P. anaerobius* was grown overnight at 37 °C under anaerobic conditions in an anaerobic jar in Wilkins-Chalgren anaerobe broth with N-azidoacetylglucosamine tetraacylated at a final concentration of 100 µM or with D-galactose as a control. Bacteria were spun down and washed three times in 1× PBS supplemented with 1% BSA. The final pellet was resuspended in 500 µl of 1% BSA in 1× PBS plus 5 µl of 2 mM Click-iT Alexa Fluor 488 sDIBO. Tubes were incubated (with rocking and protected from light) for 2 h, after which bacteria were pelleted and washed five times with 3% BSA in 1× PBS. After a final wash, bacteria were resuspended in 1× PBS and were used for co-culture with Caco-2 cells for live imaging analysis. Live imaging was acquired with a fluorescence microscope (Leica).

TEM. Approximately 1 × 10⁶ colonic cells were grown in a 6-well plate co-cultured with bacteria for 1 h (MOI = 10) and then fixed in 2.5% glutaraldehyde. Fixed cell samples were further fixed using 1% osmium tetroxide, followed by dehydration with an increasing concentration gradient of ethanol and propylene oxide. Samples were then embedded, cut into 50-nm sections, and stained with 3% uranyl acetate and lead citrate. Images were acquired with a Philips CM100 Transmission Electron Microscope (FEI).

Far-western assay. The far-western assay was performed as described previously³³. To prepare the biotinylated HT-29 cell surface proteins, HT-29 cells were first labelled with 1 mM EZ-Link Sulfo-NHS-LC-Biotin (Thermo Fisher Scientific) for 2 h at 4 °C; then surface proteins were extracted with PBS containing 1% Triton X-100 (Sigma-Aldrich) for 1 h at room temperature, followed by centrifugation. Then, whole-cell *P. anaerobius* proteins were extracted with PBS containing 1% Triton X-100, separated by SDS–polyacrylamide gel electrophoresis (PAGE) and transferred onto a polyvinylidene difluoride (PVDF) membrane. The PVDF membrane was blocked with 5% BSA for 1 h and incubated with biotinylated HT-29 surface proteins overnight at 4 °C. Biotin-labelled proteins were detected using avidin-conjugated horseradish peroxidase (HRP). The corresponding bands in SDS–PAGE were excised for identification by mass spectrometry. As a control, the PVDF membrane was incubated with avidin-conjugated HRP without pre-incubation with biotinylated HT-29 surface proteins.

Biotin pull-down assay. The biotin pull-down assay was performed using the Biotinylated Protein Interaction Pull-Down Kit (Thermo Fisher Scientific) according to the manufacturer's instructions. Briefly, HT-29 or Caco-2 cells were labelled with 1 mM EZ-Link Sulfo-NHS-LC-Biotin at 4 °C for 2 h; then, surface proteins were extracted with 1% Triton X-100 in PBS for 1 h at room temperature. The *P. anaerobius* surface membrane proteins were also extracted with 1% Triton X-100 in PBS for 1 h at room temperature. To perform the binding assay, the biotinylated HT-29 or Caco-2 surface proteins were incubated with streptavidin agarose resin for 4 h at 4 °C. After washing three times with wash buffer, the resins were incubated overnight at 4 °C with *P. anaerobius* surface membrane proteins. The resins were then washed three times and incubated with elution buffer for 5 min, followed by centrifugation. Eluted proteins were subjected to SDS–PAGE and visualized by silver staining. The corresponding bands were identified by mass spectrometry. As a negative control, streptavidin agarose resin was incubated with non-biotinylated HT-29 or Caco-2 surface proteins.

GST pull-down assay. To generate the recombinant GST–PCWBR2 protein, the *Pcwr2* gene (GenBank: AMEL01000018.1) was cloned into the pGEX-4T1 vector and transformed into *E. coli* Rosetta 2-competent cells. The transformed bacteria were then inoculated into lysogeny broth and grown at 37 °C for 2.5–3 h when the optical density reached 0.4–0.6. Isopropyl-β-D-thiogalactoside was added to get a final concentration of 1 mM to induce the expression of the recombinant proteins at 25 °C. After overnight expression, the bacterial pellets were collected, suspended in PBS and lysed with 1 mg ml⁻¹ lysozyme by incubating the cells on ice for 1 h. The supernatant containing the GST–PCWBR2 proteins was collected after centrifugation at 4 °C for 15 min at 20,000 g and for the GST pull-down assay. To perform the GST pull-down assay, GST–PCWBR2 was incubated with GST agarose beads (GE Healthcare), followed by adding membrane proteins from colonic cells or recombinant human integrin α_v/β₁ proteins (R&D systems) overnight at 4 °C. The beads were then washed and boiled with SDS–PAGE gel loading buffer. Eluted proteins were separated by SDS–PAGE and analysed by silver staining or western blot.

RNA-seq. Approximately 1 × 10⁶ colonic cells were grown in a 6-well plate co-cultured with bacteria for 4 h (MOI = 100) under anaerobic conditions. After washing with PBS, total RNA was extracted with TRIzol reagent (Thermo Fisher Scientific). RNA-seq was performed by Beijing Novogene Technology. Pathway

enrichment analysis was performed using gene set enrichment analysis (Broad Institute). Datasets were analysed using the hallmark gene sets database to identify upregulated cellular pathways. The enrichment score was calculated by member genes ranking at the top of the ranked gene list with 1,000 permutations. The maximum gene set size was fixed at 500 genes and the minimum size was fixed at 15 genes. Gene sets with a *q* < 0.25 false discovery rate were selected for pathway enrichment.

Western blot. The total proteins isolated from cells or tissue samples and protein concentration were measured by DC Protein Assay (Bio-Rad Laboratories); 10 µg of protein from each sample were separated on 10% SDS–PAGE and then transferred onto PVDF membranes. After blocking with 5% BSA, blots were incubated with the primary antibodies listed in Supplementary Table 6 overnight at 4 °C and secondary antibodies for 1 h at room temperature, respectively. Membranes were exposed to Pierce ECL Western Blotting Substrate (GE Healthcare). Band intensities were determined using ImageJ (National Institutes of Health).

Gene expression profiling analyses. Total RNA was extracted from cell pellets or colonic tissues using the TRIzol reagent. Complementary DNA was synthesized from 1 µg of total RNA using the PrimeScript RT–PCR Kit (Takara). The mouse inflammatory response and autoimmunity PCR array (PAMM-077Z; QIAGEN) was used to analyse colonic tumours from mice treated with or without *P. anaerobius*. The qPCR primers used for validation are listed in Supplementary Table 5.

Integrin α_v/β₁ knockdown. Control siRNA and siRNA targeting integrin α_v (siITGA2) were purchased from Thermo Fisher Scientific. The validated siRNA (no. S7537) and integrin β₁ (siITGB1 homo-859) sequence is GCACCAGCCCAUUUAGCUATT; 10 nM of siRNA were transfected into cells using Lipofectamine 2000 (Thermo Fisher Scientific) according to the manufacturer's instructions.

Multicolour flow cytometry analysis of tumour-associated immune cells. Multicolour flow cytometry was performed to study the immune cell types in the colonic mucosae of *Apc*^{Min/+} mice. Colon samples were dissected and incubated in Hank's balanced salt solution with 0.1 mg ml⁻¹ collagenase D (Roche) and 50 U ml⁻¹ DNase I (Roche) for 30 min at 37 °C on a shaking platform. The solution containing the digested tumours was filtered through a 70 µm cell strainer and centrifuged at 400 g for 5 min. For cell surface staining, cells were incubated with Fc blocking antibody (BioLegend) for 15 min and stained with fluorochrome-conjugated monoclonal antibodies of cell surface markers (Supplementary Table 6). For intracellular cytokine IL-7a staining, cells were stimulated for 4 h in Roswell Park Memorial Institute complete medium with 50 ng ml⁻¹ phorbol 12-myristate 13-acetate (Abcam) and 50 ng ml⁻¹ ionomycin (Abcam) in the presence of 5 µg ml⁻¹ brefeldin A (BioLegend). Then, cells were stained with cell surface markers, fixed with the FOXP3 Fix/Perm Buffer Set (BioLegend), permeabilized with FOXP3 Perm buffer (BioLegend) according to the manufacturer's recommendations and stained with intracellular cytokine IL-7a antibody. For FOXP3 staining, cells were stained with cell surface markers, fixed and permeabilized with the FOXP3 Fix/Perm Buffer Set, and then stained with anti-FOXP3 antibodies (BioLegend; Supplementary Table 6). Cells were also stained in parallel with the respective control isotype antibodies. Flow cytometry was performed using BD FACSAria Fusion Flow Cytometry Cell Sorter (BD Biosciences) and the data was analysed with the FlowJo v.9 software (FlowJo LLC).

Ki-67 immunohistochemistry. Ki-67 staining was performed on paraffin-embedded colon sections. The cell proliferation index was determined by counting the proportion of cells that stained positive for Ki-67. At least 1,000 cells were counted in 5 random microscopic fields.

Statistical analysis. A Mann–Whitney *U*-test or Student's *t*-test was performed to compare the variables of the two sample groups. The difference in cell growth curves was determined with two-way analysis of variance. Data are expressed as the mean ± s.d. or mean ± s.e.m. as indicated in the figure legends. Statistical tests were two-tailed and *P* < 0.05 was considered as statistically significant.

Reporting Summary. Further information on research design is available in the Nature Research Reporting Summary linked to this article.

Data availability

All datasets and raw data generated and/or analysed during the current study are available from the corresponding author upon reasonable request. The RNA-seq data are deposited with the NCBI with accession code [PRJNA544569](https://www.ncbi.nlm.nih.gov/submit/PRJNA544569).

Received: 20 August 2018; Accepted: 17 July 2019;
Published online: 9 September 2019

References

1. Ferlay, J. et al. Cancer incidence and mortality worldwide: sources, methods and major patterns in GLOBOCAN 2012. *Int. J. Cancer* **136**, E359–E386 (2015).
2. Nistal, E., Fernández-Fernández, N., Vivas, S. & Olcoz, J. L. Factors determining colorectal cancer: the role of the intestinal microbiota. *Front. Oncol.* **5**, 220 (2015).
3. Zeller, G. et al. Potential of fecal microbiota for early-stage detection of colorectal cancer. *Mol. Syst. Biol.* **10**, 766 (2014).
4. Sobhani, I. et al. Microbial dysbiosis in colorectal cancer (CRC) patients. *PLoS ONE* **6**, e16393 (2011).
5. Yu, J. et al. Metagenomic analysis of faecal microbiome as a tool towards targeted non-invasive biomarkers for colorectal cancer. *Gut* **66**, 70–78 (2017).
6. Nakatsu, G. et al. Gut mucosal microbiome across stages of colorectal carcinogenesis. *Nat. Commun.* **6**, 8727 (2015).
7. Rakoff-Nahoum, S. & Medzhitov, R. Regulation of spontaneous intestinal tumorigenesis through the adaptor protein MyD88. *Science* **317**, 124–127 (2007).
8. Shen, X. J. et al. Molecular characterization of mucosal adherent bacteria and associations with colorectal adenomas. *Gut Microbes* **1**, 138–147 (2010).
9. Wang, T. T. et al. Structural segregation of gut microbiota between colorectal cancer patients and healthy volunteers. *ISME J.* **6**, 320–329 (2012).
10. Zackular, J. P. et al. The gut microbiome modulates colon tumorigenesis. *mBio* **4**, e00692-13 (2013).
11. Wu, S. G. et al. A human colonic commensal promotes colon tumorigenesis via activation of T helper type 17 T cell responses. *Nat. Med.* **15**, 1016–U64 (2009).
12. Kostic, A. D. et al. *Fusobacterium nucleatum* potentiates intestinal tumorigenesis and modulates the tumor-immune microenvironment. *Cell Host Microbe* **14**, 207–215 (2013).
13. Rubinstein, M. R. et al. *Fusobacterium nucleatum* promotes colorectal carcinogenesis by modulating E-cadherin/ β -catenin signaling via its FadA adhesin. *Cell Host Microbe* **14**, 195–206 (2013).
14. Humphries, J. D., Byron, A. & Humphries, M. J. Integrin ligands at a glance. *J. Cell Sci.* **119**, 3901–3903 (2006).
15. Louis, P., Hold, G. L. & Flint, H. J. The gut microbiota, bacterial metabolites and colorectal cancer. *Nat. Rev. Microbiol.* **12**, 661–672 (2014).
16. Murphy, E. C. & Frick, I. M. Gram-positive anaerobic cocci: commensals and opportunistic pathogens. *FEMS Microbiol. Rev.* **37**, 520–553 (2013).
17. Tsoi, H. et al. *Peptostreptococcus anaerobius* induces intracellular cholesterol biosynthesis in colon cells to induce proliferation and causes dysplasia in mice. *Gastroenterology* **152**, 1419–1433 (2017).
18. Xia, H., Nho, R. S., Kahm, J., Kleidon, J. & Henke, C. A. Focal adhesion kinase is upstream of phosphatidylinositol 3-kinase/Akt in regulating fibroblast survival in response to contraction of type I collagen matrices via a β_1 integrin viability signaling pathway. *J. Biol. Chem.* **279**, 33024–33034 (2004).
19. Reif, S. et al. The role of focal adhesion kinase-phosphatidylinositol 3-kinase-Akt signaling in hepatic stellate cell proliferation and type I collagen expression. *J. Biol. Chem.* **278**, 8083–8090 (2003).
20. Gabrilovich, D. I., Ostrand-Rosenberg, S. & Bronte, V. Coordinated regulation of myeloid cells by tumours. *Nat. Rev. Immunol.* **12**, 253–268 (2012).
21. Movahedi, K. et al. Identification of discrete tumor-induced myeloid-derived suppressor cell subpopulations with distinct T cell-suppressive activity. *Blood* **111**, 4233–4244 (2008).
22. Kim, J. & Bae, J. S. Tumor-associated macrophages and neutrophils in tumor microenvironment. *Mediators Inflamm.* **2016**, 6058147 (2016).
23. Grivennikov, S. I. et al. Adenoma-linked barrier defects and microbial products drive IL-23/IL-17-mediated tumour growth. *Nature* **491**, 254–258 (2012).
24. Irrazábal, T., Belcheva, A., Girardin, S. E., Martin, A. & Philpott, D. J. The multifaceted role of the intestinal microbiota in colon cancer. *Mol. Cell* **54**, 309–320 (2014).
25. Bridgewater, R. E., Norman, J. C. & Caswell, P. T. Integrin trafficking at a glance. *J. Cell Sci.* **125**, 3695–3701 (2012).
26. Watarai, M., Funato, S. & Sasakawa, C. Interaction of Ipa proteins of *Shigella flexneri* with $\alpha_5\beta_1$ integrin promotes entry of the bacteria into mammalian cells. *J. Exp. Med.* **183**, 991–999 (1996).
27. Vanhaesebroeck, B., Guillermet-Guibert, J., Graupera, M. & Bilanges, B. The emerging mechanisms of isoform-specific PI3K signalling. *Nat. Rev. Mol. Cell Biol.* **11**, 329–341 (2010).
28. Gabrilovich, D. I. & Nagaraj, S. Myeloid-derived suppressor cells as regulators of the immune system. *Nat. Rev. Immunol.* **9**, 162–174 (2009).
29. Liu, Y. & Cao, X. The origin and function of tumor-associated macrophages. *Cell. Mol. Immunol.* **12**, 1–4 (2015).
30. Swamy, M. V. et al. Chemoprevention of familial adenomatous polyposis by low doses of atorvastatin and celecoxib given individually and in combination to APC^{Min} mice. *Cancer Res.* **66**, 7370–7377 (2006).
31. Letourneau, J., Levesque, C., Berthiaume, F., Jacques, M. & Mourez, M. In vitro assay of bacterial adhesion onto mammalian epithelial cells. *J. Vis. Exp.* **16**, 2783 (2011).
32. Geva-Zatorsky, N. et al. In vivo imaging and tracking of host-microbiota interactions via metabolic labeling of gut anaerobic bacteria. *Nat. Med.* **21**, 1091–1100 (2015).
33. Han, Y. W. et al. Identification and characterization of a novel adhesin unique to oral fusobacteria. *J. Bacteriol.* **187**, 5330–5340 (2005).

Acknowledgements

This project was supported by the Science and Technology Program Grant Shenzhen (no. JCYJ20170413161534162), HMRF Hong Kong (no. 17160862), a grant from the Faculty of Medicine CUHK on Microbiota Research, RGC-GRF Hong Kong (nos. 14111216 and 14163817), a Vice-Chancellor's Discretionary Fund CUHK (no. 4930711), and the Shenzhen Virtual University Park Support Scheme to the CUHK Shenzhen Research Institute.

Author contributions

X.L. performed the cell line and mice experiments and drafted the manuscript. L.T., E.S.H.C., C.H.S. and M.Y.Y.G. performed the mice experiments. C.C.W. revised the manuscript. O.O.C. analysed the RNA-seq data. A.W.H.C. analysed the H&E staining data. F.K.L.C. and J.J.Y.S. commented on the study. J.Y. designed and supervised the study and revised the manuscript.

Competing interests

The authors declare no competing interests.

Additional information

Supplementary information is available for this paper at <https://doi.org/10.1038/s41564-019-0541-3>.

Reprints and permissions information is available at www.nature.com/reprints.

Correspondence and requests for materials should be addressed to J.Y.

Publisher's note: Springer Nature remains neutral with regard to jurisdictional claims in published maps and institutional affiliations.

© The Author(s), under exclusive licence to Springer Nature Limited 2019

Reporting Summary

Nature Research wishes to improve the reproducibility of the work that we publish. This form provides structure for consistency and transparency in reporting. For further information on Nature Research policies, see [Authors & Referees](#) and the [Editorial Policy Checklist](#).

Statistical parameters

When statistical analyses are reported, confirm that the following items are present in the relevant location (e.g. figure legend, table legend, main text, or Methods section).

n/a Confirmed

- ☐ ☒ The exact sample size (n) for each experimental group/condition, given as a discrete number and unit of measurement
- ☐ ☒ An indication of whether measurements were taken from distinct samples or whether the same sample was measured repeatedly
- ☐ ☒ The statistical test(s) used AND whether they are one- or two-sided
Only common tests should be described solely by name; describe more complex techniques in the Methods section.
- ☒ ☐ A description of all covariates tested
- ☒ ☐ A description of any assumptions or corrections, such as tests of normality and adjustment for multiple comparisons
- ☐ ☒ A full description of the statistics including central tendency (e.g. means) or other basic estimates (e.g. regression coefficient) AND variation (e.g. standard deviation) or associated estimates of uncertainty (e.g. confidence intervals)
- ☒ ☐ For null hypothesis testing, the test statistic (e.g. F , t , r) with confidence intervals, effect sizes, degrees of freedom and P value noted
Give P values as exact values whenever suitable.
- ☒ ☐ For Bayesian analysis, information on the choice of priors and Markov chain Monte Carlo settings
- ☒ ☐ For hierarchical and complex designs, identification of the appropriate level for tests and full reporting of outcomes
- ☒ ☐ Estimates of effect sizes (e.g. Cohen's d , Pearson's r), indicating how they were calculated
- ☐ ☒ Clearly defined error bars
State explicitly what error bars represent (e.g. SD, SE, CI)

Our web collection on [statistics for biologists](#) may be useful.

Software and code

Policy information about [availability of computer code](#)

Data collection

QuantStudio™ 7 Flex System (Thermo Fisher Scientific), FACS Diva 6.1.3 (BD Biosciences), Philips CM100 transmission electron microscope (FEI, Hillsboro, OR),

Data analysis

FlowJo (v9), Image J 1.51, Prism v6

For manuscripts utilizing custom algorithms or software that are central to the research but not yet described in published literature, software must be made available to editors/reviewers upon request. We strongly encourage code deposition in a community repository (e.g. GitHub). See the Nature Research [guidelines for submitting code & software](#) for further information.

Data

Policy information about [availability of data](#)

All manuscripts must include a [data availability statement](#). This statement should provide the following information, where applicable:

- Accession codes, unique identifiers, or web links for publicly available datasets
- A list of figures that have associated raw data
- A description of any restrictions on data availability

The datasets generated during and/or analysed during the current study are available from the corresponding authors upon request.

Field-specific reporting

Please select the best fit for your research. If you are not sure, read the appropriate sections before making your selection.

☒ Life sciences ☐ Behavioural & social sciences ☐ Ecological, evolutionary & environmental sciences

For a reference copy of the document with all sections, see [nature.com/authors/policies/ReportingSummary-flat.pdf](https://www.nature.com/authors/policies/ReportingSummary-flat.pdf)

Life sciences study design

All studies must disclose on these points even when the disclosure is negative.

Sample size	See the statistics analysis in the methods
Data exclusions	NA
Replication	All experiments were repeated 3 three times as three independent experiments unless otherwise stated.
Randomization	NA
Blinding	NA

Reporting for specific materials, systems and methods

Materials & experimental systems

n/a	Involved in the study
<input checked="" type="checkbox"/>	<input type="checkbox"/> Unique biological materials
<input type="checkbox"/>	<input checked="" type="checkbox"/> Antibodies
<input type="checkbox"/>	<input checked="" type="checkbox"/> Eukaryotic cell lines
<input checked="" type="checkbox"/>	<input type="checkbox"/> Palaeontology
<input type="checkbox"/>	<input checked="" type="checkbox"/> Animals and other organisms
<input checked="" type="checkbox"/>	<input type="checkbox"/> Human research participants

Methods

n/a	Involved in the study
<input checked="" type="checkbox"/>	<input type="checkbox"/> ChIP-seq
<input type="checkbox"/>	<input checked="" type="checkbox"/> Flow cytometry
<input checked="" type="checkbox"/>	<input type="checkbox"/> MRI-based neuroimaging

Antibodies

Antibodies used	Supplementary Table 6 provided with manuscript contains information on all antibodies used in the study
Validation	The antibodies were all commercially available and validated by respective companies

Eukaryotic cell lines

Policy information about [cell lines](#)

Cell line source(s)	Colon cancer cell lines HT-29 , Caco-2 and SW48 were obtained from ATCC. Colon normal immortalized epithelial cell line NCM460 was obtained from INCELL
Authentication	The cell lines were bought from ATCC and INCELL with authentication
Mycoplasma contamination	None of the cell lines were mycoplasma contamination
Commonly misidentified lines (See ICLAC register)	None

Animals and other organisms

Policy information about [studies involving animals](#); [ARRIVE guidelines](#) recommended for reporting animal research

Laboratory animals	Description of research mice used for experiments can be found in the relevant figure legends and Methods.
--------------------	--

Wild animals

NA

Field-collected samples

NA

Flow Cytometry

Plots

Confirm that:

- ☒ The axis labels state the marker and fluorochrome used (e.g. CD4-FITC).
- ☒ The axis scales are clearly visible. Include numbers along axes only for bottom left plot of group (a 'group' is an analysis of identical markers).
- ☒ All plots are contour plots with outliers or pseudocolor plots.
- ☒ A numerical value for number of cells or percentage (with statistics) is provided.

Methodology

Sample preparation

Sample preparation listed in Methods

Instrument

BD FACSAria Fusion

Software

BD FACSDiva and FlowJo V9

Cell population abundance

Tumor infiltrating CD45 positive cells from each mice colon (20000-50000 cells) were used to further identify different kinds of immune cells by its surface markers.

Gating strategy

Relevant gating strategies shown in Supplementary Information

- ☒ Tick this box to confirm that a figure exemplifying the gating strategy is provided in the Supplementary Information.